

R1STM: One-class Support Tensor Machine with Randomised Kernel

Sarah M. Erfani* Mahsa Baktashmotlagh[†] Sutharshan Rajasegarar[‡] Vinh Nguyen*
Christopher Leckie* James Bailey* Kotagiri Ramamohanarao*

Abstract

Identifying unusual or anomalous patterns in an underlying dataset is an important but challenging task in many applications. The focus of the unsupervised anomaly detection literature has mostly been on vectorised data. However, many applications are more naturally described using higher-order tensor representations. Approaches that vectorise tensorial data can destroy the structural information encoded in the high-dimensional space, and lead to the problem of the curse of dimensionality. In this paper we present the first unsupervised tensorial anomaly detection method, along with a randomised version of our method. Our anomaly detection method, the *One-class Support Tensor Machine (1STM)*, is a generalisation of conventional one-class Support Vector Machines to higher-order spaces. 1STM preserves the multiway structure of tensor data, while achieving significant improvement in accuracy and efficiency over conventional vectorised methods. We then leverage the theory of nonlinear random projections to propose the *Randomised 1STM (R1STM)*. Our empirical analysis on several real and synthetic datasets shows that our R1STM algorithm delivers comparable or better accuracy to a state-of-the-art deep learning method and traditional kernelised approaches for anomaly detection, while being approximately 100 times faster in training and testing.

1 Introduction

Unsupervised anomaly detection plays a significant role in a wide variety of applications in terms of identifying unusual patterns in the underlying data. Relevant applications include areas as diverse as intrusion detection, fault diagnosis, health monitoring and event detection in sensor networks. Most anomaly detection techniques, such as One-class Support Vector Machines (1SVMs) [17], assume that data are encoded in first-order (vector) or second-order (matrix) tensor spaces. However, in many real-world applications data are represented more naturally as higher-order tensors. For example, sensor data are often organised into the three modes of location, type, and time, while videos are represented as 3D objects corresponding to concatenated frames over time. In this paper, we address the problem of unsupervised

anomaly detection for higher-order tensor representations that retain the intrinsic structure of the data.

Multiway tensors are natural generalisations of vectors (and matrices) and have been a growing topic of research. In particular, tensorial representations of data retain the underlying structural information of the high-dimensional space from which the data was drawn. In contrast, conventional anomaly detection techniques need to vectorise (or flatten) the different dimensions and reshape the data as high dimensional vectors. This can raise the problem of the *curse of dimensionality* for such techniques, and also results in *overfitting* when the number of training samples is small [4]. Moreover, tensor representations can preserve higher-order correlations among the modes of the data. Exploiting the original tensor data representations can result in more accurate and interpretable results [8]. Converting higher-order tensors into vectors can destroy such important structural information. For example, in a video object the multiway tensor data structure retains the relationship between the modes corresponding to the horizontal and vertical dimensions of video frame, as well as time. A higher-order anomaly detection method can then identify anomalous video objects w.r.t. these three modes. In purely vector-based anomaly detectors, each frame is represented as an independent vector, losing the notion of time (i.e., the frame order). If each frame is analysed independently of other frames, low levels of noise can cause a frame to be misclassified as an anomaly. Hence, it is highly desirable to retain the multiway data structure, and devise an anomaly detection algorithm that can be applied to the original tensor representation rather than vectorised records. The major challenge in tensor learning is to generate a model that retains the structure of the data.

Over the last decade several solutions have been proposed to extend support vector machines to tensor space, i.e., so-called Support Tensor Machines (STMs) that take a tensor as input. Earlier works on STMs [3, 21] focused on extending classical linear SVMs [4, 18] to higher-order tensors. In addition to imposing the assumption of linearly separable data, they used an iterative solution that reduces to a non-convex optimisation problem. These shortcomings were addressed by

*Department of Computing and Information Systems, The University of Melbourne, Australia. {sarah.erfani, vinh.nguyen, caleckie, baileyj, kotagiri}@unimelb.edu.au

[†]Department of Science and Engineering, Queensland University of Technology, Australia. m.baktashmotlagh@qut.edu.au

[‡]School of Information Technology, Deakin University, Australia. sutharshan.rajasegarar@deakin.edu.au

Signoretto et al. [19], who introduced a kernel-based framework that unfolds the tensor data and exploits the (unfolded) matrices to construct nonlinear kernels. Although enabling nonlinear data modelling, the unfolding stage destroys the inter-mode relationship of the multiway data. Recently, He et al. [8] proposed a structure-preserving kernel for nonlinear tensor learning, incorporating a tensor factorisation and a structure-preserving feature mapping to derive the kernel. To this end research on tensor learning has focused on supervised approaches, and to our knowledge, no research has been undertaken into *unsupervised* tensor learning.

The main objective of this work is to design an efficient unsupervised anomaly detection scheme for higher-order tensors that preserves the multiway structure of the data. Our contribution is two-fold. First, we introduce a One-class STM (1STM) for unsupervised anomaly detection that builds on ideas from [8] for incorporating tensor factorisation to leverage the tensorial representation, and nonlinear kernels. Multiway datasets are first factorised using the CAN-DECOMP/PARAFAC (CP) [10] method, and then mapped to a tensorial feature space to generate a structure-preserving higher order kernel. Our main contribution is a *randomised* 1STM (R1STM), a novel structure-preserving kernel machine using randomised nonlinear features and a linear classifier to derive a highly scalable algorithm for tensorial anomaly detection. Our extensive experiments on several benchmark and synthetic datasets show that our proposed approach substantially improves the accuracy and efficiency of anomaly detection, while maintaining the natural representation of the data. We show that this improvement is due to the combination of a *tensorial representation* with *data randomisation*, making it possible to conduct anomaly detection on large-scale data-intensive applications.

2 Related Work

The two closest relevant lines of research to our own work are tensor learning and kernel randomisation, which we briefly review in this section. Table 1 compares our work with the most relevant kernel machines.

Tensor learning: To extend SVMs to accept tensorial data input, several studies have focused on reforming the data representation, e.g., through subspace learning or tensor factorisation. Tao et al. [20] developed supervised tensor learning, a general framework that extends vector-based learning algorithms for use with tensor objects, by applying a combination of convex optimisation and multilinear operators. Later in [21], Tao et al. applied their framework to various classical SVM algorithms such as C -SVM [4] and ν -SVM

Table 1: Comparison of existing kernel machines with 1STM and R1STM.

Technique	Tensorial	Nonlinear	Unsupervised	Randomised
H1SVM [17]	N	Y	Y	N
Tao et al. [21]	Y	N	N	N
Signoretto et al. [19]	Y	Y	N	N
He et al. [8]	Y	Y	N	N
R1SVM [5]	N	Y	Y	Y
1STM	Y	Y	Y	N
R1STM	Y	Y	Y	Y

[18]. In a similar fashion, Cai et al. [3], and Wang and Chen [23] presented a support tensor machine for second-order tensors. Liu et al. [11] introduced a locally maximum margin technique for image and video classification. The key problem with [21, 3, 23, 11] is that they involve an iterative optimisation procedure, raising the problem of non-convex optimisation. Hao et al. [7] overcome this issue by reformulating the linear C -SVM model and obtained a tensor space model.

Note that all the above STMs are restricted to linear classifiers in tensor space. Most recently, [19, 8] have extended the concept of supervised tensor learning into tensor factorisations, to merge the desirable properties of kernel methods and tensor factorisations, for tensorial data that exists on a nonlinear manifold. A common approach to exploit the tensor structure with nonlinear kernel models is to use unfolded matrices to construct nonlinear kernels [19]. However, such methods only capture the relationships within each single mode of the tensor data, because the structural information about inter-mode relationships of tensor data is lost in the unfolding process. To avoid this, He et al. [8] proposed a tensor kernel that preserves tensor structures based on a dual-tensorial mapping, i.e., by mapping each tensor sample from the input space to a higher-order tensor feature space while preserving the structure.

Kernel randomisation: While numerous 1SVM formulations using nonlinear kernels have been proposed in the literature, a common feature of many formulations is the solution of a quadratic programming (QP) problem. In particular, these kernel-based methods rely on the computation of a kernel matrix over all pairs of data points, which limits the scalability of training 1SVMs on large datasets. This can also limit the effectiveness of 1SVMs on high dimensional inputs, given the need to have sufficiently large training samples spanning the variation in the high dimensional space.

Existing approaches to address the scalability problems of SVMs either preprocess the data prior to building the SVM, e.g., using dimensionality reduction techniques such as PCA or Kernel-PCA, or alleviate the QP problem of kernel machines, e.g., by breaking the problem into smaller pieces, for example by using chunking

[22], or sequential minimal optimisation [14]. A more recent trend explores the use of randomisation, such as linear random projection [2] as a substitute for the computationally expensive cost of kernel matrix construction. An early example is the work of Achlioptas et al. [1], which replaces the kernel function by a randomised kernel to speed-up KPCA. The work of Rahimi and Recht [15, 16] made a breakthrough in this approach. They replicated an RBF kernel by randomly projecting the data to a lower dimensional space and then used linear algorithms. Random projection avoids the complexity of traditional optimisation methods needed for nonlinear kernels. Recently randomisation has been applied to other kernel machines, such as dot-product kernels [9], polynomial kernels [6], and 1SVM [5].

Inspired by the idea of [8] and [15], in Section 4 we propose a model for using randomised projection in the context of unsupervised tensor learning, and propose a randomised tensorial kernel.

3 Preliminaries

3.1 Notation Throughout this paper vectors are denoted by bold, italic lower-case letters, e.g., \mathbf{x} , matrices by bold, upright capital letters, e.g., \mathbf{X} , and tensors by calligraphic letters, e.g., \mathcal{X} . Their elements are denoted by indices ranging from 1 to the capital letter of the index, e.g., $n = 1, \dots, N$. $\mathcal{X} \in \mathbb{R}^{I_1 \times \dots \times I_N}$ means \mathcal{X} is a real N^{th} -order tensor. R denotes the rank of tensor. $\|\cdot\|_F$ denotes the Frobenius norm.

3.2 Tensor Algebra

DEFINITION 3.1. (TENSOR) An N^{th} -order tensor $\mathcal{X} \in \mathbb{R}^{I_1 \times \dots \times I_N}$ is a multi dimensional array of real numbers. An element of \mathcal{X} is denoted by x_{i_1, \dots, i_N} , where $1 \leq i_n \leq I_n$, and $1 \leq n \leq N$.

DEFINITION 3.2. (TENSOR PRODUCT) The tensor product, also known as outer product, of two tensors $\mathcal{X} \in \mathbb{R}^{I_1 \times \dots \times I_N}$ and $\mathcal{Y} \in \mathbb{R}^{I'_1 \times \dots \times I'_M}$ is defined by

$$(3.1) \quad (\mathcal{X} \otimes \mathcal{Y})_{i_1, \dots, i_N, i'_1, \dots, i'_M} = x_{i_1, \dots, i_N} y_{i'_1, \dots, i'_M}$$

for all values of the indices.

DEFINITION 3.3. (INNER PRODUCT) The inner product, also known as scalar product, of two same size tensors $\mathcal{X}, \mathcal{Y} \in \mathbb{R}^{I_1 \times \dots \times I_N}$ is defined as the sum of the products of their entries:

$$(3.2) \quad \langle \mathcal{X}, \mathcal{Y} \rangle = \sum_{i_1=1}^{I_1} \dots \sum_{i_N=1}^{I_N} x_{i_1, \dots, i_N} y_{i_1, \dots, i_N}.$$

DEFINITION 3.4. (FROBENIUS NORM) The Frobenius norm of a tensor $\mathcal{X} \in \mathbb{R}^{I_1 \times \dots \times I_N}$ computes the square root of the sum of the squares of all its elements,

$$(3.3) \quad \|\mathcal{X}\|_F = \sqrt{\langle \mathcal{X}, \mathcal{X} \rangle} = \sqrt{\sum_{i_1=1}^{I_1} \dots \sum_{i_N=1}^{I_N} x_{i_1, \dots, i_N}^2}.$$

DEFINITION 3.5. (RANK-1 TENSOR) An N^{th} -order tensor \mathcal{X} has rank one if it is the tensor product of N vectors $\mathbf{u}_i \in \mathbb{R}^{I_i}$, where $1 \leq i \leq N$,

$$(3.4) \quad \mathcal{X} = \mathbf{u}^1 \otimes \dots \otimes \mathbf{u}^N = \prod_{n=1}^N \otimes \mathbf{u}^n.$$

The rank R of an N^{th} -order tensor \mathcal{X} is determined by the minimum number of rank-1 tensors that produce \mathcal{X} in a linear combination.

DEFINITION 3.6. (CP FACTORISATION) Given a tensor $\mathcal{X} \in \mathbb{R}^{I_1 \times \dots \times I_N}$, it can be factorised if it can be decomposed as rank-one tensors with length R ,

$$(3.5) \quad \mathcal{X} = \sum_{r=1}^R \mathbf{x}_r^{(1)} \otimes \dots \otimes \mathbf{x}_r^{(N)}.$$

3.3 One-class SVM (1SVM) Let $\mathbf{X} = \{x_i : i = 1, \dots, M\}$ be a set of training samples and $y_i \in \{-1, 1\}$ be their corresponding labels. In practice, \mathbf{X} is mapped from the input space \mathbb{R}^n to a feature space \mathbb{R}^H via a nonlinear function $\phi(\cdot) : \mathbb{R} \rightarrow \mathbb{R}^H$, resulting in a set of image vectors $X_\phi = \{\phi(x_i) : i = 1, \dots, M\}$. A hyperplane-based 1SVM (H1SVM) [17] aims to identify anomalies in the feature space by finding the hyperplane that best separates the data from the origin. The decision function of H1SVM returns +1 in a region where most of the data points occur (i.e., where the probability density is high), and returns -1 elsewhere. This problem can be formulated as the following quadratic optimisation function:

$$(3.6) \quad \min_{\mathbf{w}, \boldsymbol{\xi}, \rho} \quad \frac{1}{2} \|\mathbf{w}\|^2 + \frac{1}{M\nu} \sum_{i=1}^M \xi_i - \rho$$

$$\text{s.t.} \quad (\mathbf{w} \cdot \phi(\mathbf{x}_i)) \geq \rho - \xi_i,$$

$$\xi_i \geq 0, \quad \forall i = 1, \dots, M.$$

where $\nu \in (0, 1]$ is a regularisation parameter that controls the fraction of anomalies and the fraction of support vectors, and ξ_i are the slack variables that allow some of the data vectors to lie on the wrong side of the hyperplane. Since non-zero slack variables ξ_i are penalised in the objective function, the H1SVM

estimates a decision function $f(\mathbf{x}) = \text{sgn}(\mathbf{w} \cdot \phi(\mathbf{x}) - \rho)$ that maximises the distance of all the data points (in the feature space) from the hyperplane to the origin, parameterised by a weight vector \mathbf{w} and an offset ρ .

By introducing the Lagrange multipliers and setting the primal variables \mathbf{w} , ξ and ρ equal to zero, the quadratic program can be derived as the dual of the primal program in Eq. (3.6):

$$(3.7) \quad \min_{\alpha} \quad \frac{1}{2} \sum_{ij} \alpha_i \alpha_j k(\mathbf{x}_i, \mathbf{x}_j) \\ \text{s.t.} \quad 0 \leq \alpha_i \leq \frac{1}{M\nu}, \sum_i \alpha_i = 1,$$

where α_i are the Lagrange multipliers. The decision function is defined as:

$$(3.8) \quad f(\mathbf{x}) = \text{sgn}(\mathbf{w} \cdot \phi(\mathbf{x}) - \rho), \\ = \text{sgn} \left(\sum_{i=1}^M \alpha_i k(\mathbf{x}_i, \mathbf{x}) - \rho \right).$$

4 Our Approach

In this section we first introduce the 1STM and then describe our randomised tensorial kernel.

4.1 One-class Support Tensor Machine (1STM)

Let $\{\mathcal{X}_i, y_i\}$ be a pair corresponding to a training sample for *binary* classification, where $\mathcal{X}_i \in \mathbb{R}^{I_1 \times \dots \times I_N}$ is an N^{th} -order tensor and $y_i \in \{-1, 1\}$ is the corresponding label for $i = 1, \dots, M$. In [8] it was shown that the tensor binary classification problem can be modeled as a convex quadratic optimization problem in the framework of the standard nonlinear SVM. Based on this finding and the H1SVM, we present a framework for a one-class STM.

The optimization problem of binary tensor classification can be formulated as follows:

$$(4.9) \quad \min_{\mathcal{W}, b, \xi} \quad \frac{1}{2} \|\mathcal{W}\|_F^2 + C \sum_{i=1}^M \xi_i, \\ \text{s.t.} \quad y_i (\langle \mathcal{W}, \phi(\mathcal{X}_i) \rangle + b) \geq 1 - \xi_i, \\ \xi_i \geq 0, \forall i = 1, \dots, M,$$

where \mathcal{W} is the weight tensor of the separating hyperplane, C is a regularisation parameter that balances the trade-off between the classification margin and misclassification error, and b is the bias. Let ϕ be a feature mapping that maps a dataset into the Hilbert space H , given a tensor $\mathcal{X} \in \mathbb{R}^{I_1 \times \dots \times I_N}$ then

$$(4.10) \quad \phi : \mathcal{X} \rightarrow \phi(\mathcal{X}) \in \mathbb{R}^{H_1 \times \dots \times H_N}.$$

The optimisation problem in Eq. (4.9) is a generalisation of the standard nonlinear SVM. The mapping

function projects each mode of \mathcal{X} to a higher dimension called the high-dimensional tensor space. To perform anomaly detection one needs to find the hyperplane that best separates the data from the origin. In other words, the decision function in the 1STM returns +1 in the region where most of the data points occur, and returns -1 elsewhere. To separate the data set from the origin, we solve the following quadratic program:

$$(4.11) \quad \min_{\mathcal{W}, \xi, \rho} \quad \frac{1}{2} \|\mathcal{W}\|_F^2 + \frac{1}{M\nu} \sum_{i=1}^M \xi_i - \rho \\ \text{s.t.} \quad (\langle \mathcal{W}, \phi(\mathcal{X}_i) \rangle) \geq \rho - \xi_i, \\ \xi_i \geq 0, \forall i = 1, \dots, M.$$

By introducing the Lagrange multipliers, we arrive at the following quadratic problem, which is the dual of the primal problem in Eq. (4.11):

$$(4.12) \quad \min_{\alpha_1, \dots, \alpha_M} \quad \frac{1}{2} \sum_{i,j=1}^M \alpha_i \alpha_j k(\mathcal{X}_i, \mathcal{X}_j), \\ \text{s.t.} \quad 0 \leq \alpha_i \leq \frac{1}{M\nu}, \sum_{i=1}^M \alpha_i = 1.$$

Further, $\mathcal{W} = \sum_i \alpha_i \phi(\mathcal{X}_i)$. Using the Karush-Kuhn-Tucker optimality conditions (KKT conditions), tensor data can be characterised in terms of whether they fall below, above, or on the hyperplane boundary in the feature space depending on the corresponding α_i values. Tensor data with positive α_i values are the support tensors. Further, for $0 < \alpha_i < 1/M\nu$, the tensor data fall on the hyperplane and hence ρ can be recovered using these tensors, given that $\rho = \langle \mathcal{W}, \phi(\mathcal{X}_i) \rangle = \sum_j \alpha_j k(\mathcal{X}_j, \mathcal{X}_i)$. Therefore, the tensor-based decision function can be written as

$$(4.13) \quad f(\mathcal{X}) = \text{sgn} \left(\sum_{i=1}^M \alpha_i k(\mathcal{X}, \mathcal{X}_i) - \rho \right).$$

The solution to the quadratic program in Eq. (4.13) is characterised by the parameter ν , which sets an upper bound on the fraction of anomalies (training examples regarded as out-of-class) and a lower bound on the number of training examples used as support vectors.

Like other kernel machines, learning with the 1STM degenerates into computing the kernel function. A tensor dataset retains the essential information embedded in its multiway structure, therefore an important aspect of kernel learning for such complex objects is to represent them by sets of key structural features and design kernels on such sets. CP factorisation extracts a structure-preserving kernel in the tensor product feature space. In this way, each tensor object is represented

as a sum of rank-one tensors in the original space, and is then mapped to the tensor product feature space for tensor kernel learning [8].

Let $\mathcal{X} = \sum_{r=1}^R \prod_{n=1}^N \otimes \mathbf{X}_r^{(n)}$ be the CP factorisation of $\mathcal{X} \in \mathbb{R}^{I_1 \times \dots \times I_N}$. When a tensor's rank $R = 1$, the feature space tensor mapping is defined as

$$(4.14) \quad \phi : \mathcal{X}^{(n)} \rightarrow \phi(\mathcal{X}^{(n)}) \in \mathbb{R}^{H_1 \times \dots \times H_N},$$

and the kernel for two same-sized tensors \mathcal{X} and \mathcal{Y} is reduced to

$$(4.15) \quad k(\mathcal{X}, \mathcal{Y}) = \prod_{n=1}^N k(\mathbf{x}^{(n)}, \mathbf{y}^{(n)}).$$

In the case of higher-order tensors the kernel can be derived in a similar fashion. Given that the tensor feature space is a high-dimensional space of the original space, the same operations are applicable. Hence, tensor data can be factorised in the feature space, similar to the original space. Then the mapping is derived as:

$$(4.16) \quad \phi : \sum_{r=1}^R \prod_{n=1}^N \otimes \mathcal{X}^{(n)} \rightarrow \sum_{r=1}^R \prod_{n=1}^N \otimes \phi(\mathcal{X}^{(n)}).$$

This corresponds to mapping tensor data into a higher dimensional tensorial feature space and performing the factorisation in this space. Then the kernel in the higher space is just the standard inner product of the tensor data [8],

$$(4.17) \quad k \left(\sum_{r=1}^R \prod_{n=1}^N \otimes \mathbf{x}_r^{(n)}, \sum_{r=1}^R \prod_{n=1}^N \otimes \mathbf{y}_r^{(n)} \right) = \sum_{i=1}^R \sum_{j=1}^R \prod_{n=1}^N k(\mathbf{x}_i^{(n)}, \mathbf{y}_j^{(n)}).$$

Using popular kernels such as the Gaussian RBF kernel, the above equation can be formulated as:

$$(4.18) \quad k(\mathcal{X}, \mathcal{Y}) = \sum_{i=1}^R \sum_{j=1}^R \exp \left(-\sigma \sum_{n=1}^N \|\mathbf{x}_i^{(n)}, \mathbf{y}_j^{(n)}\|^2 \right).$$

However, the computational complexity of 1STM grows quadratically with the number of training samples. A linear kernel imposes linear computational complexity, but it introduces a bias to the origin. This problem can be removed by using an RBF kernel, which has a higher computational complexity associated with the higher dimensional kernels, thus making it cumbersome for processing large scale datasets.

In order to overcome this limitation, in the next subsection, we propose to exploit nonlinear random projections inside a linear 1STM, which serves as a good approximation of a nonlinear kernel.

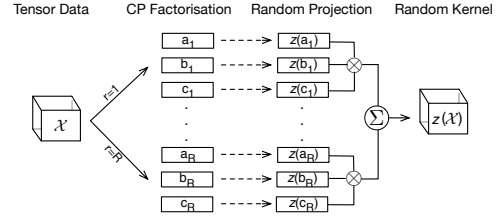


Figure 1: Random tensorial kernel.

4.2 Randomised 1STM (R1STM) We propose R1STM, a nonlinear randomised variant of our 1STM, which applies the original linear 1STM method on a randomised nonlinear projection of the tensor data. We first discuss how to generate the nonlinear random features from the original data, and then we show how to employ these features to detect anomalies using a linear machine. This approach eliminates the need to deal with large kernel matrices for large datasets, consequently reducing the computational complexity while achieving comparable detection accuracy to conventional nonlinear machines.

4.2.1 Generating Nonlinear Random Features

Consider the problem of fitting a function f to the data set $\{\mathcal{X}_i, y_i\}$, where y_i values are always set to 1 for the one-class problem. This fitting problem consists of finding f that minimises the following empirical risk

$$(4.19) \quad R^{reg}[f(\mathcal{X})] = R^{emp}[f(\mathcal{X})] + \frac{1}{2} \|f(\mathcal{X})\|_H^2$$

where $R^{emp}(\cdot)$ is the empirical risk and $\frac{1}{2} \|f(\mathcal{X})\|_H^2$ is the regulariser. The empirical risk is the average loss and can be written as

$$(4.20) \quad R^{emp}[(\mathcal{X})] \equiv \frac{1}{M} \sum_{i=1}^M l(f(\mathcal{X}_i), y_i),$$

where $l(f(\mathcal{X}_i), y_i)$ is the loss function that penalises the deviation between the prediction $f(\cdot)$ and the label y , i.e., this captures the cost of the errors caused when $f(\cdot)$ is negative on the training samples.

For the 1STM problem, the loss function $l(y, y')$ is of the form $l(y, y') = \max(0, 1 - yy')$. Using the kernel function, the function $f(\mathcal{X}) = \text{sgn}(\langle \mathcal{W}, \phi(\mathcal{X}) \rangle - \rho)$ becomes $f(\mathcal{X}) = \sum_{i=1}^M \alpha_i k(\mathcal{X}, \mathcal{X}_i)$. By jointly optimising over \mathcal{W} and α_i in a greedy manner, the solution can be found. However, this is computationally intensive. It was proven in [16] that the nonlinear optimisation problem over $(\alpha, \mathbf{w}_1, \dots, \mathbf{w}_M)$ for matrix (and vector) spaces, can be solved by randomly sampling the $\mathbf{w}_i \in \mathbb{R}^d$ from a data-independent distribution $p(\mathbf{w})$ and creating d -dimensional random features $\mathbf{z}(\mathcal{X}) = [\mathbf{z}_1 \dots \mathbf{z}_d]$,

where $\mathbf{z}_i = [\cos(\mathbf{w}_i^T \mathbf{x}_1 + b_i), \dots, \cos(\mathbf{w}_i^T \mathbf{x}_M + b_i)]$ and $\mathbf{e}_j = [\cos(\mathbf{w}_j^T \mathbf{y}_1 + b_j), \dots, \cos(\mathbf{w}_j^T \mathbf{y}_M + b_j)]$ are Fourier based random features.

In order to take advantage of this randomisation in our tensorial kernel, we use CP factorisation and randomise the rank-one tensors, as shown in Figure 1. Therefore, Eq. (4.17) is simplified to

$$(4.21) \quad k \left(\sum_{r=1}^R \prod_{n=1}^N \otimes \mathbf{x}_r^{(n)}, \sum_{r=1}^R \prod_{n=1}^N \otimes \mathbf{y}_r^{(n)} \right) = \sum_{i=1}^R \sum_{j=1}^R \prod_{n=1}^N (\mathbf{z}_i^{(n)})^T \mathbf{e}_j^{(n)}.$$

Then, we arrive at the following simplified optimisation problem:

$$(4.22) \quad \min_{\boldsymbol{\alpha} \in \mathbb{R}^d} \quad \frac{1}{M} \sum_i l(\boldsymbol{\alpha}^T \mathbf{z}_i, y_i) \\ \text{s.t.} \quad \|\boldsymbol{\alpha}\|_\infty \leq B$$

where B is a regularisation constant. Furthermore, it is shown by [16] that using randomly selected features in nonlinear spaces causes only *bounded* error compared to using optimised features:

THEOREM 4.1. *Let p be a distribution on Ω and $|\phi(\mathbf{x}; \mathbf{w})| \leq 1$. Let $\mathcal{F} = \{f(\mathbf{x}) = \int_\delta \alpha(\mathbf{w}) \phi(\mathbf{x}; \mathbf{w}) d\mathbf{w} : |\alpha(\mathbf{w})| \leq Bp(\mathbf{w})\}$. Draw $\mathbf{w}_1, \dots, \mathbf{w}_d$ iid from p . Further let $\lambda > 0$, and l be some L -Lipschitz loss function, then the function $f^*(\mathbf{x}) = \sum_{i=1}^d \alpha_i \phi(\mathbf{x}; \mathbf{w}_i)$ minimises the empirical risk $l(f^*(\mathbf{x}), y)$ has a distance from the l -optimal estimator in F bounded by:*

$$(4.23) \quad E_p[l(f^*(\mathbf{x}), y)] - \min_{f \in \mathcal{F}} E_p[l(f(\mathbf{x}), y)] \\ \leq O \left(\left(\frac{LB}{\sqrt{M}} + \frac{1}{\sqrt{d}} LB \right) \sqrt{\log \frac{1}{\delta}} \right)$$

with a probability of at least $1 - 2\delta$.

The convergence rate of our randomised R1STM to its original kernel 1STM version can be expressed by the following theorem [12]:

THEOREM 4.2. *Given the data $\mathbf{X} \in \mathbb{R}^{M \times d}$, a shift invariant kernel k , a kernel matrix $\mathbf{K}_{ij} = k(\mathbf{x}_i, \mathbf{x}_j)$ and its approximation $\hat{\mathbf{K}}$ using d random features, it can be proven that*

$$(4.24) \quad \mathbb{E} \|\hat{\mathbf{K}} - \mathbf{K}\| \leq \sqrt{\frac{3M^2 \log M}{d}} + \frac{2M \log M}{d}.$$

The proof to this theorem can be found in [12].

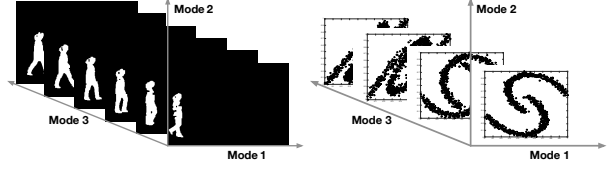


Figure 2: Illustration of third-order CASIAA and Banana datasets.

5 Empirical Analysis

In this section, we evaluate the performance of our 1STM and R1STM techniques with experiments on eight real dataset and two synthetic datasets. The aim of these experiments is to compare the performance of the proposed techniques in terms of accuracy and efficiency with conventional anomaly detection approaches.

Datasets: The experiments are conducted on four sensor measurement datasets¹ that are formed into third-order tensors (i.e., features×samples×time): (i) Daily and Sport Activity (DSA), (ii) Gas Sensor Arrays in Open Sampling Settings (GSAOS)², (iii) PAMAP2 Physical Activity Monitoring Dataset (PAMAP2), and (iv) University of Southern California Human Activity Dataset (UHAD); and four gait datasets (v) University of South Florida Gait (USFG) including 3 gait recognition datasets with 32, 64 and 128 number of features, and (vi) dataset A from CASIA gait recognition³ (CASIAA). We also use a synthetic dataset known as (vii) Banana dataset, which is a mixture of two banana shaped distributions. The components of these two datasets are randomly moved in any two modes. Table 2 summarises more details about these datasets, and Figure 2 shows two examples of tensorial representations of the CASIAA and Banana datasets.

Baseline methods: To evaluate the performance and efficiency of 1STM and R1STM, we compare them with the following unsupervised baseline methods:

(i) H1SVM [17]: a hyperplaned based 1SVM with RBF kernel, one of the most prevalent anomaly detection techniques.

(ii) R1SVM (Randomised 1SVM) [5]: our work on 1SVMs with randomised kernels, replacing nonlinear kernels with random features and a linear classifier.

(iii) DRDAE (Deep Recurrent Denoising Autoencoder) [13]: a recurrent implementation of a state-of-the-art deep learning technique known as a Denoising Autoencoder. Since all of the datasets are time series, it is interesting to compare our approaches with an ef-

¹Datasets i–iii are from the UCI repository, and dataset iv is from <http://sipi.usc.edu/HAD/>.

²The original GSAOS dataset contains about 2 million features, but in this study only the first 13800 features were used.

³http://www.cbsr.ia.ac.cn/users/szheng/?page_id=71

Table 2: Details of datasets.

Dataset	Banana	DSA	GSAOS	PAMAP2	UHAD	USFG32	USFG64	USFG3128	CASIAA
Features	$80 \times 80 \times 20$	$125 \times 45 \times 60$	$150 \times 92 \times 50$	$52 \times 100 \times 50$	$6 \times 600 \times 5$	$32 \times 22 \times 10$	$64 \times 44 \times 20$	$128 \times 88 \times 20$	$240 \times 352 \times 15$
Objects	500	152	360	344	168	731	731	731	1162

Table 3: Comparison of AUC, training and test time (in seconds) of 1STM and R1STM with conventional anomaly detection techniques.

Dataset	H1SVM			DRDAE			R1SVM			1STM			R1STM		
	AUC	Train	Test	AUC	Train	Test	AUC	Train	Test	AUC	Train	Test	AUC	Train	Test
Banana	0.78	4.77×10^5	6.65×10^3	0.98	7.69×10^2	96.48	0.98	3.21	1.16	0.93	12.43	4.35	0.98	2.11	0.91
DSA	0.84	8.04×10^3	6.73×10^2	0.98	6.15×10^2	8.12	0.98	0.56	0.06	0.98	0.27	0.13	0.99	0.09	0.04
GSAOS	0.83	1.70×10^3	6.01×10^2	0.98	3.49×10^2	10.09	0.99	0.21	0.03	0.96	0.45	0.22	0.99	0.05	0.02
PAMAP2	0.90	2.07×10^5	6.23×10^3	0.96	4.87×10^2	52.02	0.96	1.38	0.29	0.97	2.72	1.43	0.98	0.51	0.24
UHAD	0.85	2.97×10^4	1.56×10^3	0.96	2.05×10^2	21.19	0.96	0.10	0.02	0.95	0.41	0.20	0.99	0.14	0.07
USFG32	0.86	2.23×10^5	4.33×10^3	0.97	4.83×10^2	61.00	0.96	1.62	0.68	0.93	7.32	2.92	0.99	1.36	0.58
USFG64	0.87	2.94×10^5	4.86×10^3	0.97	5.08×10^2	69.41	0.97	1.69	0.74	0.94	8.01	3.46	0.99	1.52	0.71
USFG128	0.88	4.18×10^5	5.37×10^3	0.97	5.63×10^2	87.32	0.97	1.83	0.85	0.96	8.12	3.94	0.99	1.71	0.80
CASIAA	0.81	5.32×10^5	7.75×10^3	0.98	1.21×10^3	1.35×10^2	0.96	6.06	2.16	0.95	18.21	5.14	0.98	3.01	1.12
Average	0.86	2.32×10^5	3.57×10^3	0.97	5.76×10^3	60.10	0.97	1.85	0.67	0.95	6.44	2.42	0.99	1.14	0.50

fective sequential data modeling technique, which combines the multiple levels of representation.

Experimental setup: All the records in each dataset are normalised between $[0,1]$, and mixed with 5% anomalous objects, randomly drawn from $U(0,1)$. All the hyper-parameters in our learning models, comprising the width ν ($0 - 1$) and gamma g ($-4 - 4$) for H1SVM, the learning rate ($0.001 - 0.1$), number of epochs ($10 - 200$), and number of hidden units ($h \ll n$) for the autoencoder, and the rank R ($1 - 12$) for CP factorisation [7, 8], are selected through grid search based on the best performance on a validation set. Note that training is performed in an unsupervised way, and labels are only used for testing.

Metrics: The Receiver Operating Characteristic (ROC) curve and the corresponding Area Under the Curve (AUC) are used to measure the accuracy of all the methods. The reported training/testing times are in seconds based on experiments run on a machine with an Intel(R) Core(TM) i7 CPU at 3.60 GHz and 16 GB RAM. For 1SVM based methods LIBSVM was used.

5.1 Performance Evaluation Table 3 shows the performance results and their average over all the datasets. The best case, i.e., the *highest* AUC and *lowest* training/test time, for each dataset is stressed through **bold-face**. The reported time only includes the training and test time of the studied models, and no preprocessing time, e.g., data vectorisation or factorisation, has been included. Section 5.3 analyses the preprocessing stage of 1STM and R1STM. For ease of interpreting the reported results, Figure 3 graphically demonstrates the average rankings of the three metrics, AUC, training and test time, obtained from Friedman’s test. As shown in this graph, R1STM delivers the best

Table 4: Wilcoxon test to compare the performance of the studied methods regarding the p -values. W^+ corresponds to the sum of the ranks for the method on the left, and W^- for the right. The W values in bold indicate that the null hypothesis is rejected for the corresponding method.

Method	Accuracy			Training Time			Test Time		
	W^+	W^-	p	W^+	W^-	p	W^+	W^-	p
R1STM vs. 1STM	45	0	0.0039	0	45	0.0039	0	45	0.0039
R1STM vs. R1SVM	28	1	0.0156	1	44	0.0078	5	40	0.0391
R1STM vs. DRDAE	28	0	0.0156	0	45	0.0039	0	45	0.0039
R1STM vs. 1SVM	45	0	0.0039	0	45	0.0039	0	45	0.0039
1STM vs. R1SVM	2.5	33.5	0.0391	43	2	0.0117	45	0	0.0039
1STM vs. DRDAE	2	26	0.0313	0	45	0.0039	0	45	0.0039
1STM vs. 1SVM	36	0	0.0078	0	45	0.0039	0	45	0.0039
R1SVM vs. DRDAE	1.5	4.5	0.7500	0	45	0.0039	0	45	0.0039
R1SVM vs. 1SVM	45	0	0.0039	0	45	0.0039	0	45	0.0039
DRDAE vs. 1SVM	45	0	0.0039	0	45	0.0039	0	45	0.0039

performance both in terms of accuracy and efficiency.

A statistical analysis is performed to explore the effect of tensor representation and randomisation on these results, and also to assess the statistical significance of the performance of the various methods. For this purpose, we perform pairwise comparisons between different methods using the Wilcoxon signed-rank test. The test returns a p -value associated with each comparison, representing the lowest level of significance of a hypothesis that results in a rejection. This value allows one to determine whether two algorithms have significantly different performance and to what extent. For all the comparisons in this study the significance level α is set to 0.05. Table 4 summarises the output of this comparison on all the performance results from Table 3.

Comparing 1STM with H1SVM, a significant boost is obtained in both accuracy and efficiency revealing the beneficial effect of the tensorial representation. Similar results are achieved when using randomisation, i.e., R1SVM vs. H1SVM, but the best result occurs

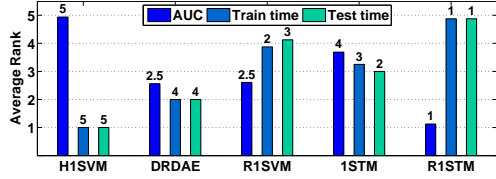


Figure 3: Comparison of rankings of anomaly detection methods for 3 metrics. The bars represent average rankings based on the Friedman test, and the number on the top of the bars indicates the ranking of the algorithm, from the best (1) to worst (5) for each given measure, and if a tie occurs then the best mean result is taken. The ranking is determined for all datasets and finally an average is calculated as the mean of all rankings.

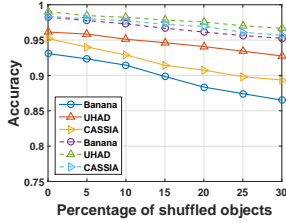


Figure 4: Comparison of accuracy with respect to increasing the percentage of shuffled objects. The solid and lines present the results for 1STM and the dotted lines present for R1STM.

when using the tensorial representation in conjunction with randomisation. The p -values in the comparison of R1STM with 1STM and R1SVM, reject the null hypothesis for the accuracy and efficiency measures with a level of significance of $\alpha = 0.05$, implying a significant improvement of R1STM over the two other methods.

5.2 Effect of Tensorial Representation The main objective of the tensor representation of data is to retain the natural structure and correlation of the records. To study this effect on 1STM and R1STM, we shuffled the third order (sequence) of some of the test objects in the Banana, UHAD and CASIAA datasets. As shown in Figure 4, the accuracy of the tensor machines decreases as the percentage of the shuffled objects increases.

That is, existing techniques have a fatal modelling flaw in that they fail to capture the inherent sequential nature of data and treat the inputs as bags of randomly permutable items agnostic to any sequential structure. This modelling property essentially suggests that the test objects could be randomly shuffled and still result in the same object. To overcome this limitation, a tensor representation is proposed to faithfully represent the spatio-temporal dependencies in the data.

5.3 Rank Sensitivity Evaluation The optimal rank R of CP factorisation is conventionally found through grid search, but it is important to determine the sensitivity of this parameter in training 1STM and

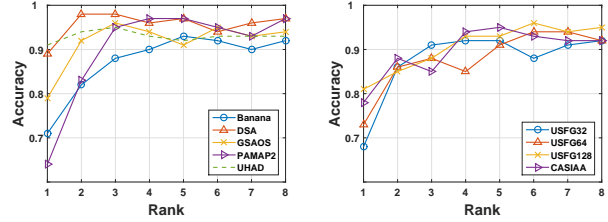


Figure 5: Comparison of accuracy with respect to increasing number of CP ranks R .

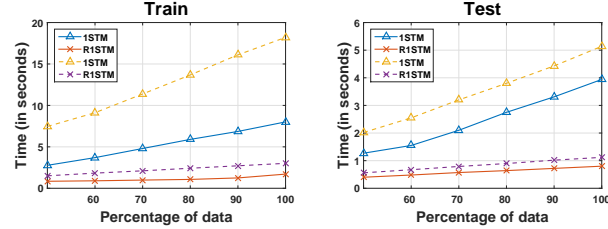


Figure 6: Comparison of accuracy with respect to increasing the percentage of sample objects. The solid dotted lines present the results for USF128 and CASIAA dataset, respectively.

R1STM. Deliberate adjustment of R is important since it plays a significant role in the performance of the algorithms. Moreover, a higher value of R indicates a higher number of items, and correspondingly a higher training/test time of the model. Figure 5 shows the results of our experiments conducted on all the datasets to measure the sensitivity of 1STM to R . As can be seen in this figure, the optimal value of R for 1STM is quite data dependent, it varies from one to the other. In this experiment, the range of $R \in [1, 12]$ were considered, but since no improvement was observed for values larger than 8, only the results from the range of $R \in [1, 8]$ were reported. In the range of $R \in [1, 2]$, R1STM delivers the AUC values presented in Table 3. For higher values of R , the AUC value slightly fluctuates (about 1%), hence no figure was included for R1STM. Table 5 compares the factorisation time of 1STM and R1STM. From this experiment it can be concluded that although CP factorisation adds an extra parameter to the list of grid-search, the optimal value of R lies in a narrow range, especially in the case of R1STM.

5.4 Scalability Evaluation A desirable property of an anomaly detection method, in addition to accuracy, is its efficiency and scalability. The computational and memory complexity of 1STM and R1STM are $O(DM^2R^2)$ and $O(dMR)$, respectively, where $D = \prod_{n=1}^N I_n$, $d = \prod_{n=1}^N J_n$, and $J_n \ll I_n$. The scalability comparison of these two algorithms on two largest datasets, CASIAA and USF128, suggests that the training/testing time of the randomised methods, unlike

Table 5: Comparison of CP decomposition time (in seconds) for 1STM and R1STM.

Dataset	1STM	R1STM	Dataset	1STM	R1STM
Banana	112.09	38.14	USFG32	76.58	6.89
DSA	11.18	8.03	USFG64	131.74	17.67
GSAOS	36.83	19.73	USFG3128	273.25	76.03
PAMAP2	137.87	36.05	CASIAA	647.45	123.11
UHAD	16.28	8.78			

1STM, grow linearly at a fairly low rate, see Figure 6.

6 Conclusions and Future Work

In this paper we have introduced two unsupervised tensorial anomaly detection methods, 1STM and R1STM, that directly apply to tensor objects and retain the data’s structure. 1STM is an extension of the conventional one-class SVMs to tensor space. R1STM, additionally, approximates the nonlinear tensorial kernel through applying the original linear classifier method on a randomised nonlinear projection of the data. Our empirical analysis on several benchmark and synthetic datasets shows that 1STM and R1STM not only maintain the data’s structure, but also they deliver significant improvements over conventional anomaly detection methods — especially R1STM, which achieves better or comparable performance to a state-of-the-art deep recurrent autoencoder, while reducing its training and testing time by more than two orders of magnitude.

References

- [1] Dimitris Achlioptas, Frank McSherry, and Bernhard Schölkopf. Sampling techniques for kernel methods. In *Advances in Neural Information Processing Systems (NIPS)*, 2002.
- [2] Avrim Blum. Random projection, margins, kernels, and feature-selection. In *Subspace, Latent Structure and Feature Selection*, pages 52–68. 2006.
- [3] Deng Cai, Xiaofei He, Ji-Rong Wen, Jiawei Han, and Wei-Ying Ma. Support tensor machines for text categorization. Technical Report 2714, University of Illinois at Urbana-Champaign, 2006.
- [4] Corinna Cortes and Vladimir Vapnik. Support-vector networks. *Machine Learning*, 20(3):273–297, 1995.
- [5] Sarah M. Erfani, Mahsa Baktashmotlagh, Sutharshan Rajasegarar, Shanika Karunasekera, and Chris Leckie. R1SVM: a randomised nonlinear approach to large-scale anomaly detection. In *Twenty-Ninth Conference on Artificial Intelligence (AAAI)*, 2015.
- [6] Raffay Hamid, Ying Xiao, Alex Gittens, and Dennis DeCoste. Compact random feature maps. In *International Conference on Machine Learning (ICML)*, 2014.
- [7] Zhifeng Hao, Lifang He, Bingqian Chen, and Xiaowei Yang. A linear support higher-order tensor machine for

- classification. *IEEE Transactions on Image Processing*, 22(7):2911–2920, 2013.
- [8] Lifang He, Xiangnan Kong, S Yu Philip, Ann B Regin, Zhifeng Hao, and Xiaowei Yang. Dusk: A dual structure-preserving kernel for supervised tensor learning with applications to neuroimages. In *SIAM International Conference on Data Mining (SDM)*, 2014.
- [9] Purushottam Kar and Harish Karnick. Random feature maps for dot product kernels. In *International Conference on Artificial Intelligence and Statistics (AISTATS)*, 2012.
- [10] Tamara G Kolda and Brett W Bader. Tensor decompositions and applications. *SIAM Review*, 51(3):455–500, 2009.
- [11] Yang Liu, Yan Liu, and Keith CC Chan. Tensor-based locally maximum margin classifier for image and video classification. *Computer Vision and Image Understanding*, 115(3):300–309, 2011.
- [12] David Lopez-Paz, Suvrit Sra, Alex Smola, Zoubin Ghahramani, and Bernhard Schölkopf. Randomized nonlinear component analysis. In *International Conference on Machine Learning (ICML)*, 2014.
- [13] Andrew L Maas, Quoc V Le, Tyler M O’Neil, Oriol Vinyals, Patrick Nguyen, and Andrew Y Ng. Recurrent neural networks for noise reduction in robust ASR. In *INTERSPEECH*, 2012.
- [14] John C Platt. Fast training of support vector machines using sequential minimal optimization. In *Advances in Kernel Methods*, pages 185–208, 1999.
- [15] Ali Rahimi and Benjamin Recht. Random features for large-scale kernel machines. In *Advances in Neural Information Processing Systems (NIPS)*, 2007.
- [16] Ali Rahimi and Benjamin Recht. Weighted sums of random kitchen sinks: Replacing minimization with randomization in learning. In *Advances in Neural Information Processing Systems (NIPS)*, 2009.
- [17] Bernhard Schölkopf, John C Platt, John Shawe-Taylor, Alex J Smola, and Robert C Williamson. Estimating the support of a high-dimensional distribution. *Neural Computation*, 13(7):1443–1471, 2001.
- [18] Bernhard Schölkopf, Alex J Smola, Robert C Williamson, and Peter L Bartlett. New support vector algorithms. *Neural Computation*, 12(5):1207–1245, 2000.
- [19] Marco Signoretto, Lieven De Lathauwer, and Johan AK Suykens. A kernel-based framework to tensorial data analysis. *Neural Networks*, 24(8):861–874, 2011.
- [20] Dacheng Tao, Xuelong Li, Weiming Hu, Stephen Maybank, and Xindong Wu. Supervised tensor learning. In *IEEE International Conference on Data Mining*, 2005.
- [21] Dacheng Tao, Xuelong Li, Xindong Wu, Weiming Hu, and Stephen J Maybank. Supervised tensor learning. *Knowledge & Information Systems*, 13(1), 2007.
- [22] Vladimir Naumovich Vapnik and Vladimir Vapnik. *Statistical Learning Theory*. Wiley New York, 1998.
- [23] Zhe Wang and Songcan Chen. New least squares support vector machines based on matrix patterns. *Neural Processing Letters*, 26(1):41–56, 2007.